IEEE Access
Multidisciplinary ⋮ Rapid Review ⋮ Open Access Journal

Received March 29, 2022, accepted April 6, 2022, date of publication April 12, 2022, date of current version April 19, 2022.

Digital Object Identifier 10.1109/ACCESS.2022.3166904

Wireless Sensor Network Dependable Monitoring for Urban Air Quality

HUYNH A. D. NGUYEN, (Member, IEEE), AND QUANG P. HA, (Senior Member, IEEE)
School of Electrical and Data Engineering, Faculty of Engineering and Information Techonology, University of Technology Sydney, Ultimo, NSW 2007, Australia

Corresponding author: Huynh A. D. Nguyen (huynhanhduy.nguyen@uts.edu.au)

This work was supported in part by the University of Technology Sydney under Project PRO19-7375, and in part by the Technology for Urban Liveability Program.

ABSTRACT This paper presents an Internet of Things-enabled low-cost wireless sensor network with newly-developed dependable schemes to improve reliability for monitoring air quality in suburban areas. The system features sensing units for router communications with energy savings from dynamic conservation. Based on the reliability function and mean time to failure, a continuous time Markov chain model is used to analyze the monitoring performance. The proposed dependable monitoring network is shown to achieve high availability with regards to energy consumption and data assurance with the survival probability of over 80% during a minimum period of 72-hour operation for monitoring air quality in a suburb. Distributions of fine particle concentrations studied over a 6-month period demonstrate feasibility of the developed system in its high correlations to benchmark monitoring stations with the Pearson's coefficients obtained at 0.903 and 0.817 respectively for PM2.5 and PM10. Statistical analysis is conducted for performance evaluation in association with two extreme events, one with bushfires and the other with pandemic lockdown. The results obtained indicate enhancements in reliability and accuracy of the colocated dependable low-cost sensors network proposed for wireless monitoring of air quality in urban conditions.

INDEX TERMS Low-cost wireless sensor networks, Internet of Things, air quality, dependability, monitoring systems.

I. INTRODUCTION

A recent projection by the United Nations (UN) foresees that by 2050 nearly 70% of global population will be living in the cities [1]. This urbanization trend leads to considerable demands for transportation, industrial production, infrastructure and energy. This would raise concerns on sustainable development and require the need for effective measures for environmental monitoring in urban areas. Interdisciplinary and transdisciplinary efforts embracing advances in information and communication technology (ICT), autonomous systems, data science, computer science, systems theory, the Internet-of-Things (IoT) and artificial intelligence (AI) have formed the basis for smart sustainable city development [2].

Towards environmental sustainability and social resilience in metropolitan areas, it is essential for residents to have clean air. In this regard, technical measures are needed for monitoring and improving air quality, whereby IoT-enabled wireless sensors networks are promising among available monitoring systems for healthy built environment and air quality management. As an example, in a crowdsourcing and cross-sector collaboration project, namely AIR Louisville [3], electronic inhaler sensors with the IoT technology have been used to provide the health data as well as environmental values for policy recommendation on air pollution management and control. An integrated monitoring system is proposed in [4] for a smart building, where real-time indoor air quality data are monitored round the clock using IoT-enabled multisensor fusion.

For outdoor air quality, a simulation model is used in [5] to monitor the traffic conditions of urban road networks that have a direct effect on vehicle emissions. An open online database and measured data from urban sensor networks has been used to address individual incidents related to air pollutants [6]. At a larger scale collaboration, the iSCAPE (Improving the Smart Control of Air Pollution in Europe), an allied project covering six cities in different European countries, has demonstrated advancements in the deployment of low-cost wireless sensor networks (LWSN) at citizens' households to enhance awareness of sustainable environment [7]. In Australia, along with recent big projects for infrastructure development to meet the urbanization needs,

The associate editor coordinating the review of this manuscript and approving it for publication was Eyhab Al-Masri.

the problem of air quality modelling and control is also of top priority [8]. A network of KOALA (Knowing Our Ambient Local Air Quality) low-cost sensors has been implemented for high spatial resolution air quality monitoring to successfully observe the emissions of fine particles and carbon monoxide during six months before and after a big sports event [9]. These initiatives show benefits and feasibility of a low-cost solution using wireless sensor networks for monitoring air pollution and improving air quality in cities.

While global smart city development can offer various dimensions and services covering all aspects of municipal activities, it should be people-centric, addressing directly citizens' well-being and quality of life [10]. Therefore, the needs and preferences of citizens should be considered in public-involved programs to implement of LWSN for environment monitoring. As reported in [11], residents may raise concerns on data quality, system reliability, operating support, ownership and the arrangement of power supply for monitoring systems installed at some locations in suburbs. Moreover, network security and data preservation should be taken into account when crowdsourcing data, e.g. in healthcare [12] or life basic necessities [13]. Indeed, low-cost sensors networks using the IoT technology can be considered as promising in environmental monitoring, e.g. for real-time urban microclimate analysis [14]. In climate and atmospheric sciences, this crowdsourcing technique, however, needs further validation and verification to become a valuable source [15]. These indicate that the IoT-enabled LWSN systems installed for urban air quality monitoring have to be accurate, reliable, and fail-safe at the first requirements.

This article aims to develop a framework of dependable low-cost wireless sensor network (DLWSN) for air quality monitoring, which addresses the affordable deployment of a colocated monitoring system for reliable data aggregation and accurate assessment of urban air quality using the IoT-enabled system with enhanced availability. Here, the reliability analysis for the proposed system is conducted via the mean time to failure (MTTF) derived from the reliability function of the monitoring system, whereby the survival and failing probabilities of its sensor modules are calculated by a Markov chain model (MCM). From the reliability analysis, a suitable configuration is selected for sensor motes supplied with a dynamic energy conservation scheme to increase the system's runtime and incorporated with a novel wireless dependable algorithm to improve the accurate, reliable and fail-safe operations of the overall system in monitoring outdoor air quality. The availability, reliability and resilience of the proposed DLWSN against environmental volatility are verified in extreme events such as bushfires and pandemic lockdown conditions. Contributions of the paper can be specified as (i) an architecture for dependable low-cost wireless sensors networks with sensor motes formed by colocated sensor modules developed from an IoT platform for urban air quality monitoring, (ii) an effective algorithm for wireless dependable monitoring to enhance system reliability, accuracy and fault-tolerance, and (iii) a promising approach to real-time urban microclimate analysis, tested in a wide range of environmental conditions.

The paper is organized as follows. After the introduction, Section 2 presents the proposed architecture for DLWSN to monitor air quality in a local area such as suburbs of a city. Section 3 is devoted to an analysis of system reliability using a continuous-time Markov chain model based on a failure rate, and presents a novel dependable monitoring algorithm. In Section 4, experiments are described, including laboratorial testing and a real-world application of the proposed DLWSN to monitor the air quality at a construction site and its surrounding area. Section 5 provides on-site results and statistical analysis to confirm the DLWSN merits, in terms of high performance in air quality monitoring, possibility for microclimate analysis, and good value for the suburban management. Finally, a conclusion is drawn in Section 6.

II. DEPENDABLE LOW-COST WIRELESS SENSOR NETWORK

The framework for the proposed low-cost wireless sensor network is introduced in this section.

A. SYSTEM DEPENDABILITY

In discrete systems, dependability is attributed to such system properties as availability, reliability, maintainability, durability and security [16]. In the context of technologies for sustainable environment, dependable systems are important for the management and information processing in various aspects of a city life, improving the citizens' responsiveness, and facilitating services and applications towards resilience of a smart city [17]. For environmental modelling, wireless sensor networks enabled in an IoT platform offer an effective tool. To deal with uncertainties associated with data collected, particular in the case of air quality monitoring, it is essential to improve accuracy, reliability and service life of these networks. To this end, we propose here the integration of dependable schemes into a LWSN for urban monitoring air pollution, in alignment with long-term development of resilient smart cities.

The early concept of dependability in IoT-enabled systems emerges in the industrial applications, which demonstrate the enhancement of the fault-safe and reliable operations in face of system's incidents or network imperfectness. It is quite often that dependable systems requires a level of redundancy, spatially or temporally, depending on the relation to sensing or communications and control. For example, the dependable control and management of solar energy in a smart building made use of redundancy in the quad controllers [18]. In wireless sensor networks, redundancy has been exploited to increase data accuracy, sensing reliability, system lifetime and security [19]. With the availability of low-cost networks, a prominent advantage coming out of redundancy is their fault-tolerant and safe operation. As such, groups of sensor motes can be colocated in clusters to extend the WSN lifetime via optimization [20], by routing adaptation (Low Energy Adaptive Clustering Hierarchy - LEACH) [21] or using fuzzy

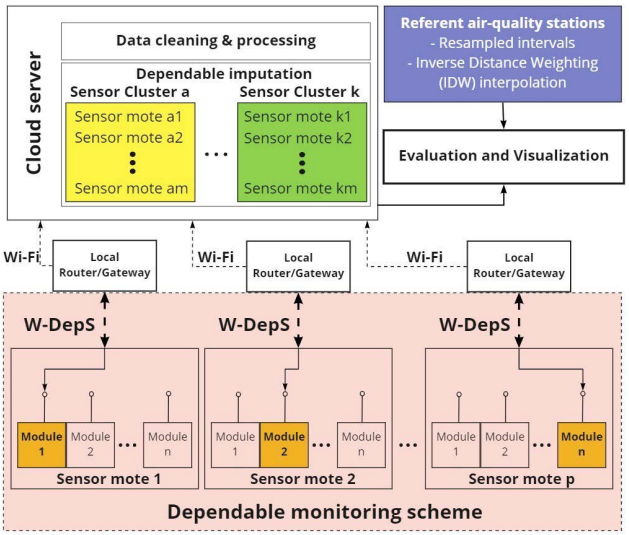

FIGURE 1. Proposed DLWSN architecture.

logic inference [22]. On the other hand, system dependability can also be achieved by increasing reliability in relation to the measurement as well as communication protocols, e.g. such as Transmission Control Protocol (TCP), Automatic Repeat Request (ARQ) or routing path, while handling possible tradeoffs at the same time with energy waste, data replication, connectivity congestion, and computational resource [23].

B. NETWORK ARCHITECTURE

Figure 1 presents the architecture of the proposed DLWSN for monitoring air pollutants in suburban areas. The system includes sensor motes of several collocated modules and local router/gateway motes to collect environmental data and transmit the most reliable values to the cloud server through a dependable monitoring scheme. There is at a time only one active sensor module in each mote (the one in orange in Fig. 1). Therein, imputed data from the sensor mote clusters are also processed and evaluated along with data obtained from nearby air-quality stations to provide accurate and reliable assessment of distributions of air pollutants at a local monitoring areas.

In the dependable scheme, each sensor module has IoT-enabled functions to measure and transmit data remotely to the sink devices (gateways/routers). As illustrated in each sensor mote in Fig. 1, the dependable monitoring schemes with developed wireless dependable sensing (W-DepS) play a role of a local manager to switch the most reliable module in a sensor mote while the other modules will stand by idly to conserve energy. The local routers are also developed to handle as an intermediate layer to transfer data between sensor motes and cloud server. However, to deal with imperfectness while transceiving high quality information from the sites, network redundancy will be integrated with physical sensor modules to formulate our dependable low-cost framework.

In this study, each sensor mote constitutes four colocated sensor modules in a quad-sensor configuration that has been field-tested on a construction site [24]. In the proposed architecture, the IoT-enabled low-cost microcontroller ESP32 is the main platform embedding our W-DepS algorithm as well as other communications and measurements. The W-DepS link is decided by a local router mote constituted by two microcontroller units (MCUs) connecting in series, in which one unit communicates with sensor modules in the local network called ESP-NOW, the remaining MCU is responsible for sending the most reliable data packets to the cloud server (internet) via the Wi-Fi network. In addition, the sensor motes can communicate directly to the cloud in cases of failing connections with the routers or for indoor applications. The on-duty (active) module selected by W-DepS will communicate for data transmission with the router, while three others are in the standby (passive) mode. Therefore, unnecessary communication and the redundant information are mitigated to improve the information utility and energy conservation in comparison to other wireless sensor networks [25]. Moreover, the supply for the sensor mote and router comes from a solar panel with proprietary lithium-powered energy storage controlled by a dynamic energy conservation scheme as described in the next section.

C. DYNAMIC ENERGY CONSERVATION FOR ENERGY SAVINGS

In environmental monitoring, wireless sensor systems often operate intermittently with low sampling frequencies (periods of minutes or hours) depending on the desired resolution. This requires the power supply for the system to be maintained over the lifespan. Here, our strategy is focused on a dynamic energy conservation (DEC) scheme, making use of the deep-sleep mode in order to extend the service time and assure stable operation of the sensor modules.

The proposed DEC scheme in each sensor module includes (i) the active state when the MCU ''wakes'' up, samples values from sensors and transmits data to gateways, and (ii) the deep-sleep mode when the MCU cuts off the power supplying to all sensors until the next self-wakeup instant. Over the active period, only the most reliable sensor module connects wirelessly to the gateways to transmit the measured data, the remaining modules send only survival states (survival probability) when having triggered signal from the local gateways. Through the W-DepS feedback, the sleeping time can be dynamically chosen and adapted by the gateways when the survival probabilities of the sensor modules become lower than a predefined threshold. From the experimental records of DEC presented in [24], the sampling interval of 15 minutes will be considered for all analysis in this paper.

The ESP-NOW network, a low-power wireless protocol in the local clusters, is deployed in our communication layers also for saving energy. This device-to-device (D2D) radio communication method allows for low-energy 2.4 GHz wireless connectivity without a common gateway like in other wireless protocols. In terms of connecting security, ESP-NOW is seamlessly integrated with CCMP (Counter Mode Cipher Block Chaining Message Authentication

Code Protocol) in combination with Primary Master Key and Local Master Key [26]. Moreover, the transmission payload can be maximum at 250 bytes and the connection range up to hundred meters in line-of-sight connectivity. Therefore, this communication protocol is an appropriate option to leverage our proposed dependable monitoring scheme for reducing the interference with the global Wi-Fi network and increasing the connectivity performance.

III. RELIABILITY ANALYSIS

Before testing and implementing the proposed DLWSN for urban air quality monitoring, an analysis of the system reliability is conducted using probability and statistics. In the IoT infrastructure, several techniques have been applied to evaluate both availability and reliability of IoT-based systems, such as the Petri net-based approach for healthcare applications [27], or the Markov chain model (MCM) for WSN deployed in areas with relatively harsh natural environments [28]. Nevertheless, most of the previous studies are limited in the virtual conditions of simulation that does not reflect the real-world application of the IoT-enabled WSN in online operation. In practice, due to the impact of volatile weather or extreme natural events on the WSN performance, the lifetime, communications and other basic functions of developed networks need to be explored in an onsite scenarios. In this work, a hierarchical MCM is proposed to derive the reliability function of colocated sensor motes using collected data from the experiments for dependability evaluation of the DLWSN.

A. RELIABILITY FUNCTION AND MEAN TIME TO FAILURE

In our dependable system, the sensor modules are colocated to measure the same environmental variables (e.g., ambient temperature, air humidity, soil moisture, air pressure, and particulate matter). In each sensor mote, only one on-duty sensor module is representative for the mote to transmit data to the intermediate gateways or directly to the server. The sensor motes are at the high-level management for data transmission, while the sensor modules are at the low level for data sensing and dependable monitoring. Hence, this configuration simplifies the embedded control algorithm in computing-constrained IoT platforms.

As the parallel-operation scheme for the colocated sensor modules is adopted, we analyze the availability and reliability for the two possible configurations, namely, (C1) all active modules operate at the same time (i.e., similar duty cycles in communication and measurement), and (C2) one at a time, i.e. one active module and the rest modules are cold-standby. To proceed with the analysis, we first assume that (i) the lifetime of a sensor mote is the time span of the maximum longevity of the whole set of modules in (C1), or the total time span of all sensor modules in a mote (C2), and (ii) a failure is caused predominantly by power exhaustion with all module batteries being discharging with the same rate.

Since the sensor modules operate with limited energy supplied by battery cells, the working status of each device should last continuously during the time. Therefore, the process involved can be represented by an exponential distribution. Moreover, the colocated sensor modules are supplied by separate power banks, hence their failures are independent and identically distributed (IID). To this end, the process can be considered as a Poisson distribution of a continuous-time Markov chain (CTMC) model. The reliability function or the so-called the survival function of module i^{th} in a sensor mote is an exponential function :

$$R_i(t) = e^{-\lambda t}, \tag{1}$$

where λ is the failing rate of module.

The reliability functions for two configurations (C1) and (C2) for a general case with n devices can be expanded respectively as,

$$R_{C1}(t) = 1 - \prod_{k=1}^{n}(1 - R_i) \tag{2}$$

and

$$R_{C2}(t) = e^{-\lambda t}\sum_{k=0}^{n-1}\frac{(\lambda t)^k}{k!}, \tag{3}$$

where k is number of failed modules at time t.

The $MTTF$, an important metric to quantify reliability of a system, is defined as [29]:

$$MTTF_{C1} = \int_0^\infty R_{C1}(t)dt = \frac{1}{\lambda}\sum_{k=1}^{n}\frac{1}{k} \tag{4}$$

and

$$MTTF_{C2} = \int_0^\infty R_{C2}(t)dt = \frac{n}{\lambda}. \tag{5}$$

It is obviously seen from (4) and (5) that the cold-standby configuration (C2) increases MTTF when higher redundant modules are in the systems (sensor motes). Hence, the reliability and survival time of systems will be higher, and our quad-sensor motes will operate with one active and three passive modules.

B. CONTINUOUS TIME MARKOV CHAIN MODEL FOR SENSOR MOTES

The CTMC model of our colocated sensors can be depicted in Fig. 2 for a sensor mote of four sensor modules with a perfect switching mechanism. Here, the working status of each sensor module of a sensor mote is represented by a state. For example, State_1 means the module 1 being in good condition and State_0 implies all the four modules not functioning and hence the mote being in the failure status. The lower layer (inside the rectangle box) demonstrates states of each sensor module by a two-state model of W and F corresponding to working and failing, respectively.

A failure of a sensor module will transit to the next state of the mote. Therefore, the transition rate between two states is assumed equally as λ_i for both the mote and the module $i-$th. The other parameter is μ_i denoting the recovery rate. This

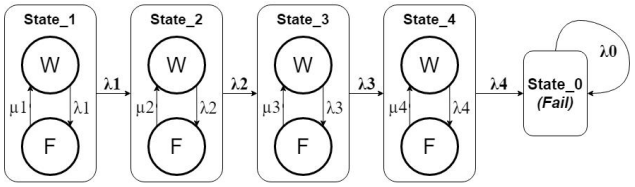

FIGURE 2. Continuous-time Markov chain model for a quad-sensor mote.

parameter is dependant on environmental changes such as solar PV panels and weather conditions. Nevertheless, as the dependable scheme can replace instantly the failing module by a working one and given a high value of the MTTF, our proposed quad-sensor configuration can assure a prolonged continuous lifetime of the proposed DLWSN.

For the onduty-standby configuration, we denote a binary variable representing the operational (active) and non-operational (standby) states of the quad-sensor mote as,

$$\pi_i = \begin{cases} 1 \rightarrow Operational \\ 0 \rightarrow Non-operational. \end{cases} \tag{6}$$

The sensor mote reliability for an n colocated sensor modules can be obtained from the combination:

$$R_{mote}(t) = \sum_{i=1}^{n} \pi_i . R_i(t), \tag{7}$$

where $R_i(t)$ is the reliability function of a sensor module.

In cluster-based networks, at least one sensor module must operate in a cluster. As such, the higher number of operational sensor modules will lead to the exponential growth to the computational latency of the network server [30]. This justifies a reasonable selection of the number n of sensor modules in a sensor mote. In this work, with $n = 4$ modules per mote, an ensemble of sensor motes will be distributed over the local area for the purpose of microclimate assessment of urban air pollution. The whole DLWSN will be controlled by the neighbour gateways to mitigate the problem of large scale implementation. The reliability of each sensor module at the lower layer is considered in the next section.

C. SENSOR MODULE RELIABILITY

As illustrated in Fig. 2, the failure of a sensor module will decide on reliability of a sensor mote. In the following, the two-state MCM is used to find the survival and failure probabilities of each sensor module at a certain time, based on the Kolmogorov forward equation as [31],

$$\dot{P}(t)^T = P(t)^T A, \tag{8}$$

or

$$[\dot{P}_F(t), \dot{P}_W(t)] = [P_F(t), P_W(t)] \begin{bmatrix} -\mu & \mu \\ \lambda & -\lambda \end{bmatrix}, \tag{9}$$

where $P(t)$ and $\dot{P}(t)$ are respectively the probability vector of all states and its time derivative, $P_W(t)$ and $P_F(t)$ are the probability of state W and state F, respectively, and A is the transition matrix of the Markov model expressed in (8). Since the module operates initially ($t = 0$) at $P_W(0) = 1$ and $P_F(0) = 0$, and given the unity sum of probabilities for all states, the following differential equations for two variables $P_W(t)$ and $P_F(t)$ are obtained as,

$$\lambda P_W(t) - \mu P_F(t) = \dot{P}_F(t) \tag{10}$$

$$P_W(t) + P_F(t) = 1. \tag{11}$$

The solution of the system (10) and (11) for each state can then be obtained [32]:

$$P_W(t) = \frac{\mu}{\mu+\lambda} + \frac{\lambda}{\mu+\lambda} e^{-(\mu+\lambda)t}, \tag{12}$$

$$P_F(t) = \frac{\lambda}{\mu+\lambda} - \frac{\lambda}{\mu+\lambda} e^{-(\mu+\lambda)t}. \tag{13}$$

The probability $P_W(t)$ is now one of the inputs in our proposed dependable scheme to determine a new active sensor module based on the potential failure from the currently operating device. In order to obtain $P_W(t)$, the two parameters, recovery rate μ and transition rate λ, have to be specified and simplified for an embedded system. In our application for air pollution monitoring at a suburb scale, the proposed DLWSN system operates with a working voltage subject to a battery threshold of $E(t) = 3.2$ V - a limit operation voltage of ESP32-MCU [26] for switching between the charge and discharge states of each module almost instantaneously. As such, when being discharged, the recovery rate (μ) can be considered zero. For the transition rate at failures, or failing rate λ, it is often taken as the reciprocal of the mean time to failure (i.e., $MTTF = 1/\lambda$) [30]. Therefore, the probability $P_W(t)$ and $P_F(t)$ can be obtained as,

$$\begin{cases} P_W(t) = e^{-\lambda t} = e^{-\frac{t}{MTTF}} \\ P_F(t) = 1 - e^{-\lambda t} = 1 - e^{-\frac{t}{MTTF}}. \end{cases} \tag{14}$$

As discussed above, the MTTF of each sensor module has its own distribution which can be sampled at a time instant t for the value of λ. The development of the proposed W-DepS is presented in the next section.

IV. SYSTEM IMPLEMENTATION AND APPLICATION

This section describes the implementation of the proposed wireless sensor network, its dependable monitoring algorithm, its laboratorial testings, and system installation for its application to air quality monitoring in a suburb.

A. DEPENDABLE MONITORING ALGORITHM

In our development, the wireless dependable monitoring algorithm is embedded in the MCUs of the gateways. These gateways are governed by the local ESP-NOW network between the sensor motes and the gateway motes, as illustrated in Fig. 1. From the ESP32-MCU, there are two integrated Xtensa 32-bit LX6 microprocessors, normally denoted as core 0 and core 1, which can work independently for multitasking by an abstract real-time operational system (i.e., FreeRTOS) to manage parallel tasks between the two cores. Fig. 3 shows the structure for task distribution and data communications between these cores (core 0 for communications

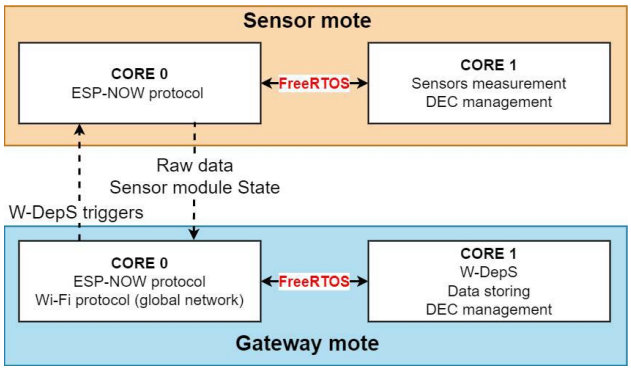

FIGURE 3. Task distribution and data communication structure.

and core 1 for other tasks). The multitasking ability allows for reduction of network interference and computational latency.

Beside raw data measured by sensors, the feedback from each sensor module includes also the probabilities of survival $P_{W_i}(t)$ and received signal strength indicators ($RSSI_i(t)$). These are sent to and stored in the gateway mote. Although the colocated sensor modules are used here, and the RSSI can be meaningful over some distance for wireless devices [33], the network's signal strength, data collection and localization are obviously affected by environmental conditions (e.g., temperature and humidity) [34]. Therefore, the RSSI can serve best as a proxy for the effects of weather volatility on the DLWSN performance. The dependable monitoring algorithm W-DepS is then developed based on status packets of the sampled probabilities and signal strength indicators. The pseudo-code of the W-DepS program is shown in Algorithm 1, wherein the output is the command for updating the reliable active module at the next cycle of the monitoring system.

Algorithm 1 W-DepS

Input : Status packets $[P_W(t), RSSI(t)]$ from sensor modules
Output: Estimate and assign the most reliable sensor module
Data: $P_W(t) = [P_{W_i}]$ and $RSSI(t) = [RSSI_i]$
Result: Identify the next active module

```
function IdentifyActive(P_Wi, RSSI_i)
    find max P_Wi with (i = 1, 2, 3, 4)
    find max RSSI_j with (j = 1, 2, 3, 4)
    if (i == j) then
        activeDevice ← i
    else if (max(P_Wi) and max(RSSI_i > min(RSSI_threshold)) then
        activeDevice ← i
    else
        activeDevice ← j
    compareLastStates(activeDevice)
end function
return updatedActiveDevice
sendControllerCommandOut(updatedActiveDevice)
```

B. LABORATORIAL TESTING RESULTS

For evaluation of the DLWN development, we have conducted laboratorial experiments to test its performance. Here, reliability for WSN can be analyzed by using modelling tools such as Reliability Block Diagram [23], Petri net [27], and Fault Tree Analysis (FTA) [35], which are convenient for simulation. However, assumptions and *a priori* parameters used in these models may not reflect well the multifaceted responses of the low-cost components of the developed WSN because of drastic changes in operational conditions or unaccountable effects in a real-world environment. Here, termination tests are laboratorially conducted to measure the MTTFs of sensor modules by setting up experiments at the intended conditions (similar data measurement, communication, sampling frequency, and energy conservation). The MTTFs are then measured from the fully-charged to failure-terminated state (power outage, system shutdown or a communications problem). Next, the probability density function (pdf) and cumulative distribution function (cdf) are modelled by using the Python reliability library [36] from the histogram of the MTTF data as shown in Fig. 4, wherein the order of legends indicates the goodness of fitted distributions from high to low. The best fit will be used for further statistical analysis.

For illustration, we consider the survival probability of twelve sensor modules to indicate a divergence in the reliability range of low-cost components. Figure 5 depicts the survival probability according to the MTTF of those tested sensor modules. The vertical dashed line marks the 72^{th} hour threshold showing that most of the modules have the probability of surviving 3 days of continuous operation to be at least 0.8, i.e. with a survival probability higher than 80%. Some other prototypes have lower survival probabilities, e.g., module 7, 8, 9, 10, and 12. As a result, the highly reliable sensor modules are selected for the real-world implementation to assure better reliability. The proposed dependable monitoring algorithm W-DepS is also tested in our laboratory with the Virtual Bench NI VB-8012 all-in-one instrument. Experiments were conducted with one master gateway module and three slave sensor modules communicating wirelessly by the ESP-NOW protocol. Figure 6 depicts the signals obtained from the all devices. A dummy program of the master device periodically switches the active slaves as can be observed by the rising and falling edges of the pulse signals with the frequency of 50 *Hz*, i.e. the red pulses with approximately 5 *V* in amplitude and 10 *ms* in width.

The blue, black and green pulses (at 3.2 V amplitude) are the responses probed from GPIOs of three slave modules when being assigned the active module by the W-DepS algorithm. These slaves are switched at a random sequence, e.g. Slave 1 → Slave 3 → Slave 2, as shown in Fig. 6. The switching duration in our experiments is approximately 1 *ms*, depending on the length of the data frame transceiving in the local network. Moreover, all three slaves toggle the GPIOs instantly ON/OFF according to the feedback signals from the master as described in Algorithm 1. The switching between

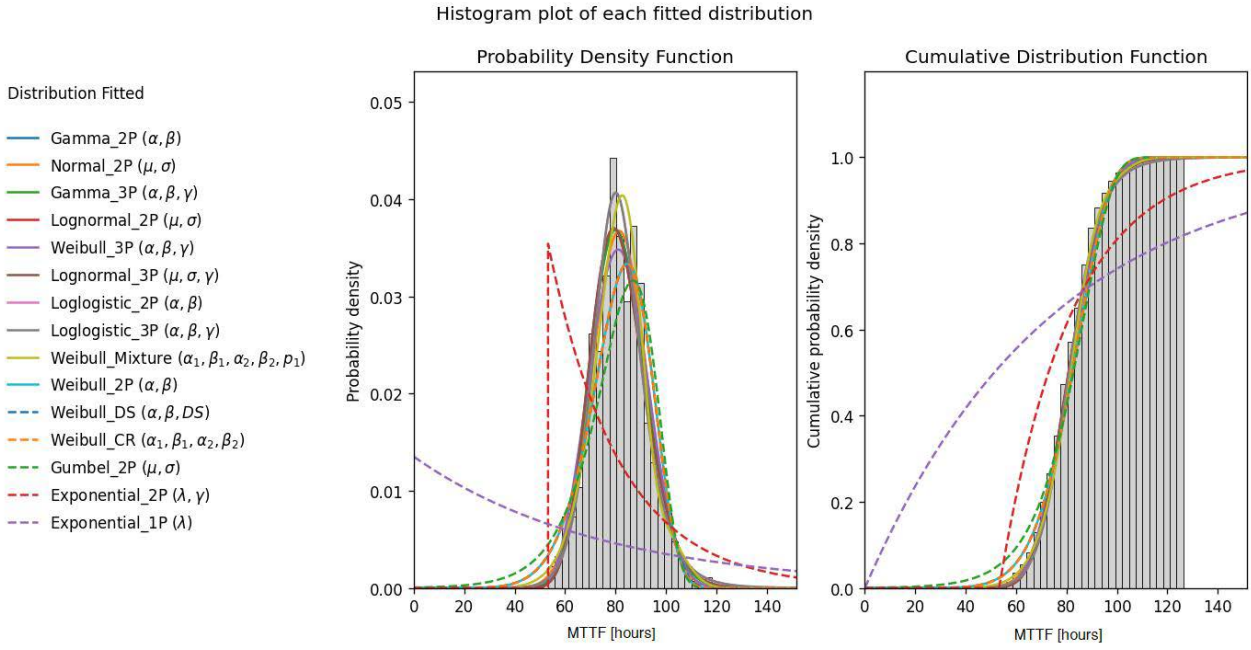

FIGURE 4. Pdf and cdf of the MTTF measured and their fitted distribution functions.

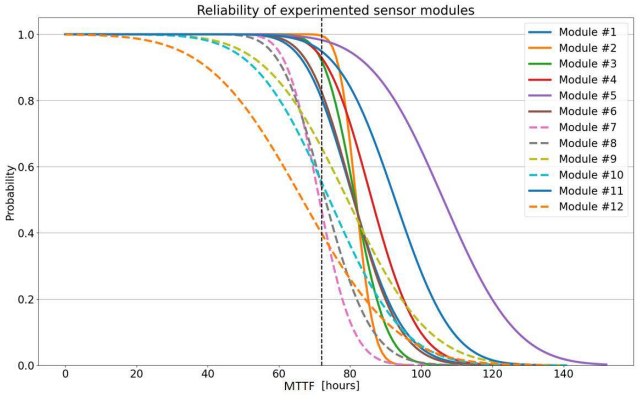

FIGURE 5. Probabilities of reliability of 12 sensor modules.

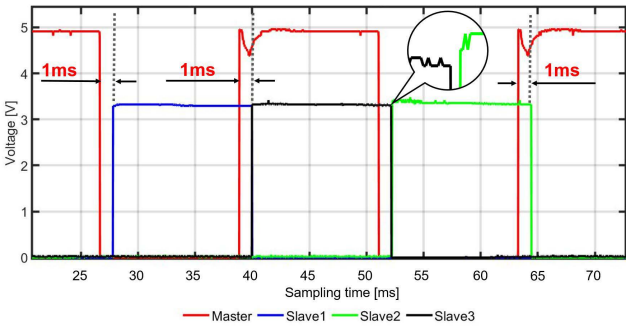

FIGURE 6. Experimental demonstration of W-DepS.

any two sensor modules takes less than one millisecond, negligible with respect to a working cycle (DEC scheme) in the range of minutes for monitoring systems. The results obtained indicate effectiveness of the proposed W-DepS algorithm along with the ESP-NOW protocol developed for the DLWSN.

C. DLWSN INSTALLATION

The study area is a construction site at coordinates $(33°49'11''S; 151°4'38''E)$, which is located approximately 17 km north-west of the Central Business District of Sydney City. Its map is depicted in Fig. 7, showing the positions of 15 developed sensor motes, denoted from T1 to T15 and surrounding suburbans having air-quality stations, namely Parramatta North, Macquarie Park, Lidcombe and Rozelle.

The area under monitoring is divided into two primary zones: (i) the on-site zone comprises sub-zones from Z1 to Z6 with motes T1-T8 spatially distributed over the construction site to monitor the impact of construction activities on suburban air quality, (ii) the off-site zone with motes T9-T15 installed in a residential area and a park in the surrounding for observing emissions from urban activities including household, transportation and any anthropogeneous sources in the area. Figure 8 depicts several sensor motes installed on electrical poles at 3 m height above the ground for proper measurement.

The monitoring period covers 6 months (from November 2019 to May 2020), associated with two important environmental events, namely a catastrophic bushfire (Black Summer) and COVID-19 lockdown, which presented different aerosol patterns in the area. In this study, the air pollutants of interest are dust emissions (particulate matters of less than 2.5 micrometers in diameter - PM2.5, and also with diameter

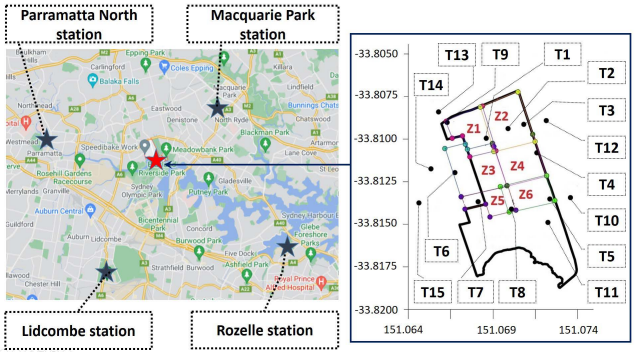

FIGURE 7. Study area and location of nearest air quality stations (left), and map of on-site sensor motes (right) with designated subzones: Z1- Site North West, Z2- Site North East; Z3- Site Mid West; Z4- Site Mid East; Z5- Site South West; Z6- Site South East.

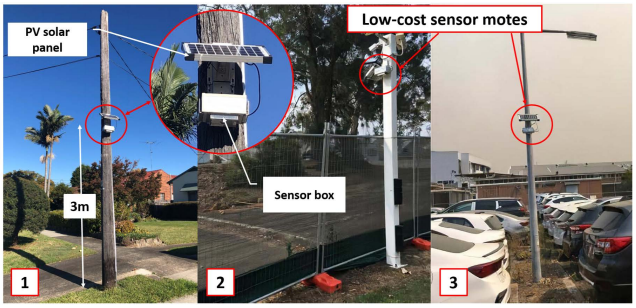

FIGURE 8. Sensor motes installed (1) T4 at a residential location, (2) T12 at the construction site, and (3) T2 in the car park.

below 10 micrometers - PM10). With the selected operational cycles of 15 minutes, over 12000 data points were collected by each sensor mote.

V. URBAN AIR QUALITY MONITORING RESULTS

This section presents the data processing and validation results with the proposed DLWSN for the real-world monitoring air quality in the mentioned suburb, along with a thorough evaluation analysis of its on-site dependability attributes through the monitoring of dust emissions from a construction site.

A. DATA PROCESSING AND VALIDATION

The data collected by the sensor motes are first compared with those provided by state-run monitoring stations close to the site as the station data are highly regarded as ground truth. They are administered by the NSW government authority and made public for various air pollutants as well as meteorological variables on the hourly and daily basis [37]. The site (Melrose Park, MP) in this study is located between Sydney Central-East and North-West regions, near several stations, of which, four air-quality stations surround MP located in Parramatta North, Macquarie Park, Lidcombe and Rozelle having the distances of approximately 7 km, 5.7 km, 7.8 km and 10.3 km, respectively, as shown in Fig. 7.

To evaluate the network performance at the MP site with reference to the four stations $S_i (i = 1, 2, 3, 4)$ in relevance to their distance, the commonly-used square inverse distance weighting (IDW) technique is applied for target point S_0 of the DLSWN:

$$\hat{y}(S_0) = \sum_{i=1}^{n} \omega_i y(S_i), \tag{15}$$

where ω_i is the weighted distance of station i^{th}, defined as:

$$\omega_i = \frac{d_{0i}^{-2}}{\sum_{i=1}^{n} d_{0i}^{-2}}, \tag{16}$$

where d_{0i} is inverse distance between station i^{th} to S_0. Raw data logged from DLWSN are first preprocessed to remove noise and anomalous values with a moving average filter by taking the average of neighbour values from left and the right as:

$$Y_{filter} = \frac{1}{n} \sum_{i=-\frac{n-1}{2}}^{\frac{n-1}{2}} y_i, \tag{17}$$

where Y_{filter} is the output of the moving average filter, and n is the range of centered samples (an odd number). Then, the Cook's distance technique is adopted in this study to identify the so-called *influence points* or outliers on the regression model:

$$D_i = \frac{\sum_{j=1}^{n} (\hat{y}_j - \hat{y}_{(j)i})^2}{p.MSE}, \tag{18}$$

where D_i is the Cook's distance of the observation i^{th}, y_i and $y_{(j)i}$ are respectively the fitted values when including and excluding samples i^{th}, MSE is the mean square error of two datasets, and p is the number of coefficients of the fitting model. Here, those samples were selected at least 3 times the means of the outliers' values.

The next step is to impute missing data by using a filtering technique [38]. Finally, as data collected by the state-run monitoring stations are available in the hourly or daily average format, the commonly-used cubic interpolation can be applied to synchronize the sampling frequency between the data from DLWSN and the station data.

The partial profiles from both datasets are presented in Fig. 9 for comparison between DWLSN data (in red) and IDW estimated data (in blue). The mean values taking over the whole period for concentrations of fine particles PM2.5 are respectively 23.73 $\mu g/m^3$ measured at MP and 24.50 $\mu g/m^3$ from stations, while those for dust PM10 at the two sources are 31.15 $\mu g/m^3$ and 49.15 $\mu g/m^3$, all within the daily national standards for particulate matter pollutants (the Australian standard thresholds are 25 $\mu g/m^3$ and 50 $\mu g/m^3$ for PM2.5 and PM10, respectively). The mean for PM2.5 are nearly equal for both sources, while those for PM10 appear to be higher from referent values than measured concentration at MP, probably because the effect of the bushfire event during that time in NSW. To evaluate the correlation of the two profiles of fine dust PM2.5, a scatter plot is also presented on the right side in Fig. 9. The Pearson's

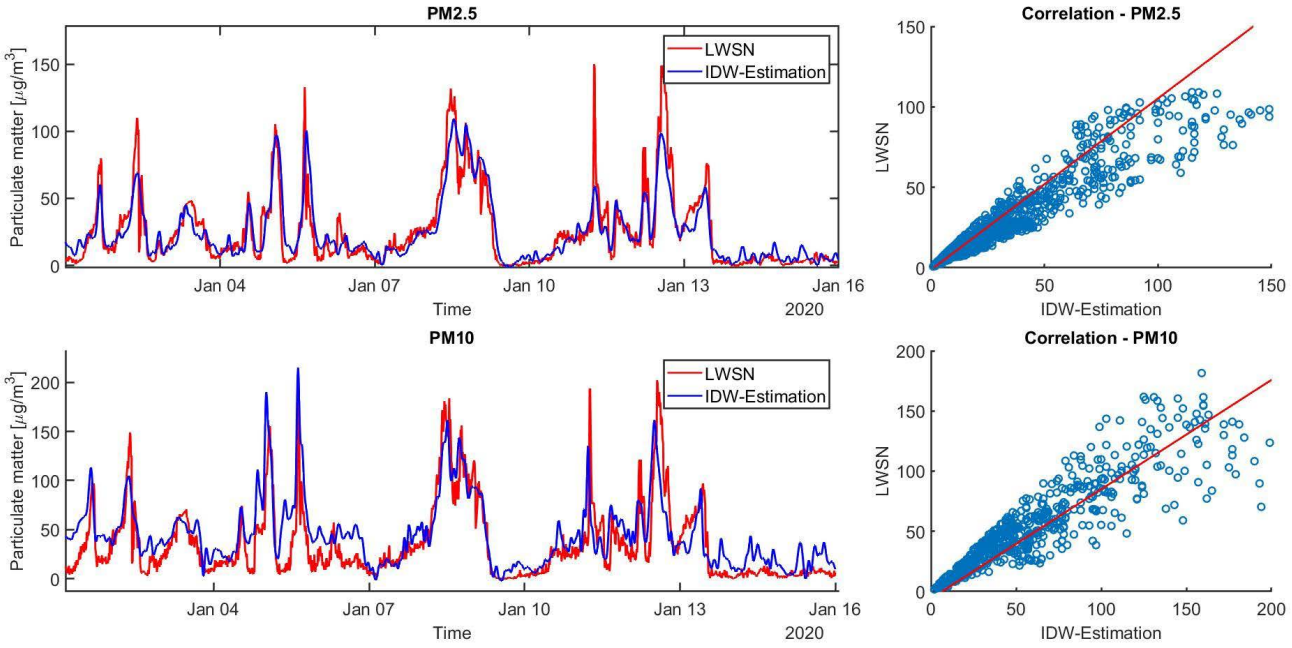

FIGURE 9. Time series of PM2.5 collected by a LWSN (Melrose Park) and estimated values from referent air-quality stations from 02nd to 16th January 2020.

correlation (r) for PM2.5 and PM10 are calculated with significant values at 0.903 and 0.817, respectively. The other statistical values such as standard deviation (STD), mean absolute error (MAE) are also given in Table 1. The statistical analysis indicates a strong correlation of the time series of particle concentrations collected by the DLWSN and those obtained at the neighbour state-run stations. Therefore, the measured data from our IoT-enabled monitoring system can be considered as accurate and reliable. The following section provides further evaluations.

B. AVAILABILITY AND RESILIENCE EVALUATION

As the survival of battery-based systems predominantly relies on duration of the solar exposure, the measured voltages of the remaining energy from each mote can indicate the availability of our system. To evaluate the DLWSN availability, we consider two practical factors (i) instant battery voltage, and (ii) daily solar exposure during the harsh condition of environment.

We consider two extreme events.

1) BLACK SUMMER BUSHFIRE

Due to the catastrophic bushfire in Black Summer beginning in early August 2019 ending in February 2020, a high level of particulate matters were distributed over a large region, including the suburb under monitoring. During that time, emissions of fine particles PM2.5 were not only from construction activities on the site but also dominantly from the wildfire, as monitored by sensor motes T2-T8 (see Fig. 7). The box plot shown in Fig. 10 summarizes statistical information of the collected data from DLWSN. Notably, the outliers

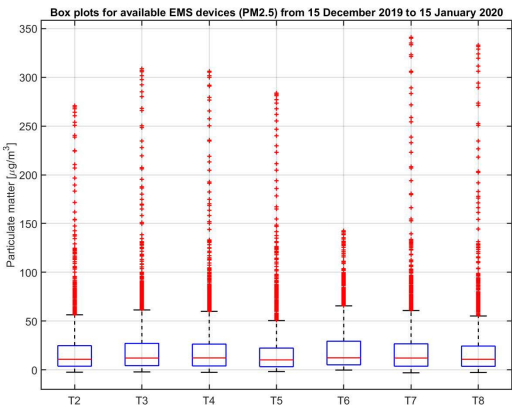

FIGURE 10. Box plots of PM2.5 by sensor motes T2-T8 implemented from November 2019 to February 2020.

of all data are quite high due to impacts of smoke and dust from the wildfire, much beyond emissions from construction activities. Notably, the outliers of T6 are relatively smaller than of the other motes, which can be explained by its location in the residential area and far way from the site.

On the other hand, the daily averages of solar exposure collected from the Bureau of Meteorology [39] along with the voltages of a sensor mote (T7) are shown typically in Fig. 11 for February 2020. During the month, the W-DepS algorithm and DEC scheme successfully selected the most reliable sensor modules while the measured voltages of sensor motes were kept around 3.95 V. During 7-9th February 2020, there was a long-awaited heavy rain in NSW, which contributed to stop the bushfire. Despite changes in the battery energy according to the level of solar exposure and the adversary

TABLE 1. Statistics of data measured from DLWSN at Melrose Park and IDW-estimation of referent stations.

Data source	Mean ($\mu g/m^3$)		STD ($\mu g/m^3$)		MAE ($\mu g/m^3$)		Pearson's correlation r	
	PM2.5	PM10	PM2.5	PM10	PM2.5	PM10	PM2.5	PM10
DLWSN	23.73	32.19	43.61	58.65	11.74	26.71	0.903	0.817
IDW-Estimation	24.50	49.15	41.19	65.58				

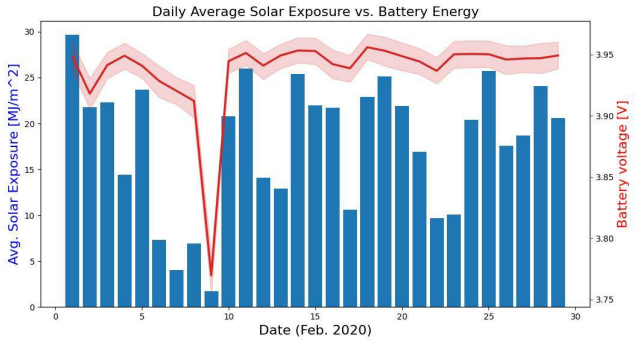

FIGURE 11. Daily average solar exposure (blue bars) and the average battery voltage (red line with min-max intervals) of the sensor mote T7 in February 2020.

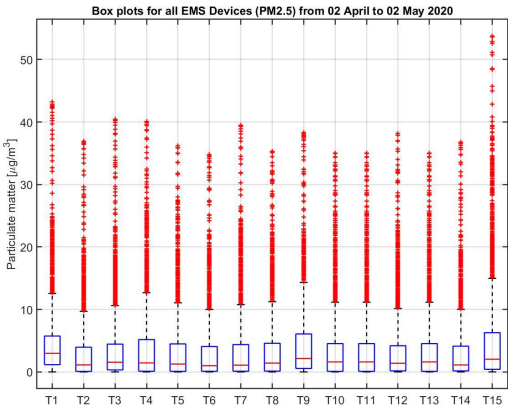

FIGURE 12. Box plots of PM2.5 by 15 sensor motes implemented from February to May 2020.

weather during the time, the voltage level recorded can drop from 3.97 V down to 3.75 V. This indicates the continuous availability as well as resilience of our DLWSN system under extreme conditions such as severe bushfires.

2) COVID-19 LOCKDOWN

Since March 2020, the whole Australia was in the lockdown due to the coronavirus pandemic (COVID-19). During the time, a decrease in anthropogeneous sources of emissions resulted in a low level of dust concentrations, as recorded from the developed LWSN. The box plots of Fig. 12 show the significant low PM2.5 concentrations measured by 15 sensor motes T1-T15 with 95% of all fine-particle levels under 20 $\mu g/m^3$. This is a direct effect of the absence of major transports in the city as well as other sources of emissions from human activities during lockdown. On the other hand, it also demonstrates accuracy and sensitivity of the proposed DLWSN for urban air quality monitoring.

C. DEPENDABILITY AND MICROCLIMATE ANALYSIS

To illustrate dependability of the proposed DLWSN, three sensor motes T1, T2 and T3 are deliberately colocated with the radial distance less than 200 m so that the environmental parameters measured in this sub-area can be considered as the same by each sensor mote. Then, the power supplying to the sensor motes was switched off deliberately to simulate failures as if caused by the adverse impacts, e.g. from damage to the physical system or any vulnerable incident. Accordingly, the following schedule applied: T1 (20^{th}-22^{nd} March), T2 (25^{th} March), T3 (28^{th} March) and later, both T3 and T1 from early April 2020. Fig. 13 presents the time series of these motes, showing missing data from them.

During the study period, T1 profile (red line) had two interruptions, during 20^{th}-22^{nd} March and after

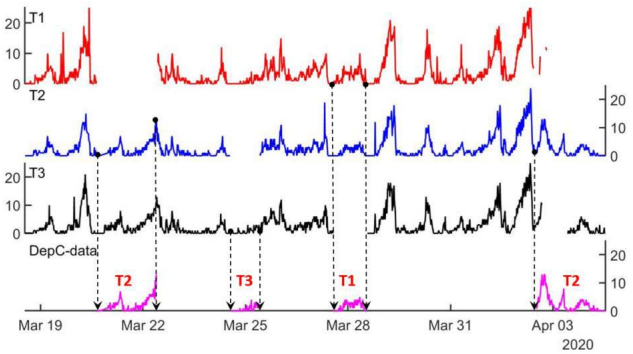

FIGURE 13. Data profiles of three low-cost sensor motes with data selection of W-DepS.

02^{nd} April 2020. Both were recognized by the W-DepS algorithm that triggered T2 (blue line) to take over as the active sensor mote in the cluster for data acquisition (magenta line). When T2 stopped operation on 25^{th} March, the algorithm compared the reliable probability between T1 and T3 (black line), and assigned the monitoring task to T3. Similarly, T1 was selected to replace T2 and T3 on 28^{th} March 2020. For the final interrupting interval, due to failures of both T3 and T1 on 3^{rd} April, values collected from T2 would be the only output of the dependable monitoring algorithm. It is clear that the W-DepS successfully handled the incidents by switching to a standby sensor mote to assure continuous monitoring in the occurence of failures in the sensor network.

Notably, an interesting advantage of the proposed DLWSN rests with its potential in environmental monitoring at a microscale, a feature exceeding the capability of state-run stations. In this study, it is used for monitoring dust emissions

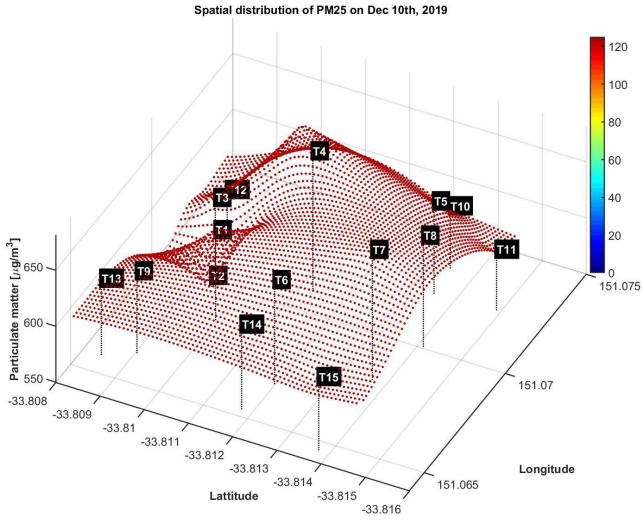

FIGURE 14. Spatial distribution of PM2.5 at midday 10^{th} December 2019.

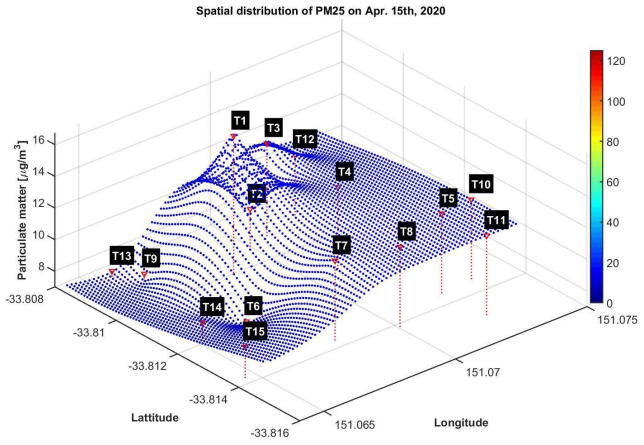

FIGURE 15. Spatial distribution of PM2.5 at midday 15^{th} April 2020.

from a construction site in a small suburb. Indeed, monitoring information can be collected at a small distance taking into account the dependability advantages of the proposed low-cost sensor networks. Typically for the two extreme events described above, the spatial distributions of PM2.5 levels on 10^{th} December 2019 and 15^{th} April 2020 at mid-day are presented respectively in Fig. 14 and Fig. 15. The dispersion of fine particles covered the site of interest using the standard color code for air quality assessment. From the spatial maps, the central area of the site (T1 - T8) have higher levels of PM2.5 in comparison with the residential (T9 - T15) due to the emissions contribution from the construction site. The results obtained are promising in microclimate analysis. Further learning schemes can help improve resilience and security of the developed network in harsh operating conditions. Those will be the topic of our future work.

VI. CONCLUSION

This paper has presented a new development for a reliable environmental monitoring system built on the combination of physical and communication redundancies. By colocation of similar sensor motes to monitor the same parameters, increasing the time to failure for each module via energy management, and incorporating an effective IoT-enabled dependable control algorithm, the proposed low-cost wireless sensor network can significantly improve the monitoring quality in terms of availability, reliability with high correlations (0.903 for PM2.5, 0.817 for PM10) and fault tolerance with a high survival probability above 80%. The continuous-time Markov model and statistical tools are utilized in the design and performance verification. The system architecture is described along with hardware implementation. The developed system has been successfully tested in laboratory conditions as well as applied to real-world monitoring of air quality profiles of a construction site in a suburb, considering the impact of construction activities as well as different weather events such as bushfires, COVID-19 lockdown and heavy rain. The obtained results show feasibility and advantageous merits for the proposed low-cost wireless sensor network for environmental monitoring, particularly for air pollution assessment. They also indicate a promising application in microclimate analysis for cities.

ACKNOWLEDGMENT

Huynh A. D. Nguyen would like to thank the Vingroup Science and Technology Scholarship Program, managed by VinUniversity and sponsored by Vingroup, for Overseas Study for Master and Doctoral degrees.

REFERENCES

[1] U. N. DESA. *2018 Revision of World Urbanization Prospects*. Accessed: May 24, 2021. [Online]. Available: https://www.un.org/development/desa/publications/2018-revision-of-world% -urbanization-prospects.html

[2] S. E. Bibri, "A foundational framework for smart sustainable city development: Theoretical, disciplinary, and discursive dimensions and their synergies," *Sustain. Cities Soc.*, vol. 38, pp. 758–794, Apr. 2018.

[3] M. Barrett, V. Combs, J. G. Su, K. Henderson, and M. Tuffli, "AIR louisville: Addressing asthma with technology, crowdsourcing, cross-sector collaboration, and policy," *Health Affairs*, vol. 37, no. 4, pp. 525–534, Apr. 2018.

[4] Q. P. Ha, S. Metia, and M. D. Phung, "Sensing data fusion for enhanced indoor air quality monitoring," *IEEE Sensors J.*, vol. 20, no. 8, pp. 4430–4441, Apr. 2020.

[5] S. S. Anjum, R. M. Noor, N. Aghamohammadi, I. Ahmedy, L. M. Kiah, N. Hussin, M. H. Anisi, and M. A. Qureshi, "Modeling traffic congestion based on air quality for greener environment: An empirical study," *IEEE Access*, vol. 7, pp. 57100–57119, 2019.

[6] L. Ricaurte, "The array of things, Chicago," *Urban Planning for Transitions*. London, U.K.: Wiley, 2021, pp. 171–182.

[7] O. González, G. Camprodon, and V. Barberán, "Sensor monitoring experiences and technological innovations," iSCAPE, Spain, Tech. Rep. D7.8, 2020.

[8] S. Metia, Q. P. Ha, H. N. Duc, and Y. Scorgie, "Urban air pollution estimation using unscented Kalman filtered inverse modeling with scaled monitoring data," *Sustain. Cities Soc.*, vol. 54, Mar. 2020, Art. no. 101970.

[9] T. Kuhn, R. Jayaratne, P. K. Thai, B. Christensen, X. Liu, M. Dunbabin, R. Lamont, I. Zing, D. Wainwright, C. Witte, D. Neale, and L. Morawska, "Air quality during and after the commonwealth games 2018 in australia: Multiple benefits of monitoring," *J. Aerosol Sci.*, vol. 152, Feb. 2021, Art. no. 105707.

[10] T. Ji, J.-H. Chen, H.-H. Wei, and Y.-C. Su, "Towards people-centric smart city development: Investigating the citizens' preferences and perceptions about smart-city services in Taiwan," *Sustain. Cities Soc.*, vol. 67, Apr. 2021, Art. no. 102691.

[11] K. Ekman and A. Weilenmann, "Behind the scenes of planning for public participation: Planning for air-quality monitoring with low-cost sensors," *J. Environ. Planning Manage.*, vol. 64, no. 5, pp. 865–882, Apr. 2021.
[12] G. Mehmood, M. Z. Khan, A. Waheed, M. Zareei, and E. M. Mohamed, "A trust-based energy-efficient and reliable communication scheme (trust-based ERCS) for remote patient monitoring in wireless body area networks," *IEEE Access*, vol. 8, pp. 131397–131413, 2020.
[13] M. Adil and M. K. Khan, "Emerging IoT applications in sustainable smart cities for COVID-19: Network security and data preservation challenges with future directions," *Sustain. Cities Soc.*, vol. 75, Dec. 2021, Art. no. 103311.
[14] P. Rathore, A. S. Rao, S. Rajasegarar, E. Vanz, J. Gubbi, and M. Palaniswami, "Real-time urban microclimate analysis using Internet of Things," *IEEE Internet Things J.*, vol. 5, no. 2, pp. 500–511, Apr. 2018.
[15] C. L. Müller, L. Chapman, S. Johnston, C. Kidd, S. Illingworth, G. Foody, A. Overeem, and R. R. Leigh, "Crowdsourcing for climate and atmospheric sciences: Current status and future potential," *Int. J. Climatol.*, vol. 35, no. 11, pp. 3185–3203, Sep. 2015.
[16] A. Avizienis, J.-C. Laprie, B. Randell, and C. Landwehr, "Basic concepts and taxonomy of dependable and secure computing," *IEEE Trans. Depend. Sec. Comput.*, vol. 1, no. 1, pp. 11–33, Jan./Mar. 2004.
[17] N. Tcholtchev and I. Schieferdecker, "Sustainable and reliable information and communication technology for resilient smart cities," *Smart Cities*, vol. 4, no. 1, pp. 156–176, Jan. 2021.
[18] Q. Ha and M. D. Phung, "IoT-enabled dependable control for solar energy harvesting in smart buildings," *IET Smart Cities*, vol. 1, no. 2, pp. 61–70, Dec. 2019.
[19] D.-I. Curiac, C. Volosencu, D. Pescaru, L. Jurca, and A. Doboli, "Redundancy and its applications in wireless sensor networks: A survey," *WSEAS Trans. Comput.*, vol. 8, no. 4, pp. 705–714, 2009.
[20] K.-C. Chu, D.-J. Horng, and K.-C. Chang, "Numerical optimization of the energy consumption for wireless sensor networks based on an improved ant colony algorithm," *IEEE Access*, vol. 7, pp. 105562–105571, 2019.
[21] Y. Xu, Z. Yue, and L. Lv, "Clustering routing algorithm and simulation of Internet of Things perception layer based on energy balance," *IEEE Access*, vol. 7, pp. 145667–145676, 2019.
[22] P. Nayak and A. Devulapalli, "A fuzzy logic-based clustering algorithm for WSN to extend the network lifetime," *IEEE Sensors J.*, vol. 16, no. 1, pp. 137–144, Jan. 2016.
[23] A. Dãmaso, N. Rosa, and P. Maciel, "Reliability of wireless sensor networks," *Sensors*, vol. 14, no. 9, pp. 15760–15785, Aug. 2014.
[24] H. A. D. Nguyen, L. V. Nguyen, and Q. P. Ha, "IoT-enabled dependable co-located low-cost sensing for construction site monitoring," in *Proc. 37th Int. Symp. Autom. Robot. Construction (ISARC)*, Oct. 2020, pp. 616–624.
[25] H. Kang, X. Li, and P. J. Moran, "Power-aware Markov chain based tracking approach for wireless sensor networks," in *Proc. IEEE Wireless Commun. Netw. Conf.*, Mar. 2007, pp. 4209–4214.
[26] Espressif Systems. *ESP32 Series the Datasheet*. Accessed: Jul. 7, 2020. [Online]. Available: https://www.espressif.com/sites/default/files/documentation/esp32_data%-sheet_en.pdf
[27] E. Andrade and B. Nogueira, "Dependability evaluation of a disaster recovery solution for IoT infrastructures," *J. Supercomput.*, vol. 76, no. 3, pp. 1828–1849, Mar. 2020.
[28] Y. Liu and Q. Zhang, "Modeling and performance optimization of wireless sensor network based on Markov chain," *IEEE Sensors J.*, vol. 21, no. 22, pp. 25043–25050, Nov. 2021.
[29] G. Yang, *Life Cycle Reliability Engineering*. Hoboken, NJ, USA: Wiley, 2007.
[30] D. Deif and Y. Gadallah, "A comprehensive wireless sensor network reliability metric for critical Internet of Things applications," *EURASIP J. Wireless Commun. Netw.*, vol. 2017, no. 1, pp. 1–18, Dec. 2017.
[31] M. Rausand and A. Høyland, *System Reliability Theory: Models, Statistical Methods, and Applications*. Hoboken, NJ, USA: Wiley, 2003.
[32] S. Ross, *Stochastic Processes*, 2nd ed. New York, NY, USA: Wiley, 1996.
[33] A. K. Paul and T. Sato, "Localization in wireless sensor networks: A survey on algorithms, measurement techniques, applications and challenges," *J. Sens. Actuator Netw.*, vol. 6, no. 4, p. 24, 2017.
[34] J. Luomala and I. Hakala, "Analysis and evaluation of adaptive RSSI-based ranging in outdoor wireless sensor networks," *Ad Hoc Netw.*, vol. 87, pp. 100–112, May 2019.
[35] I. Silva, L. A. Guedes, P. Portugal, and F. Vasques, "Reliability and availability evaluation of wireless sensor networks for industrial applications," *Sensors*, vol. 12, no. 1, pp. 806–838, Jan. 2012.
[36] M. Reid. *Reliability—A Python Library for Reliability Engineering (Version 0.7.0) [Computer Software]*. Accessed: Jul. 20, 2021. [Online]. Available: https://pypi.org/project/reliability/
[37] New South Wale Government—Planning Industry and Environment. *Search for and download air Quality Data*. Accessed: Jun. 20, 2020. [Online]. Available: https://www.dpie.nsw.gov.au/air-quality/search-for-and-download-air-quality-data
[38] S. Metia, H. A. D. Nguyen, and Q. P. Ha, "IoT-enabled wireless sensor networks for air pollution monitoring with extended fractional-order Kalman filtering," *Sensors*, vol. 21, no. 16, p. 5313, Aug. 2021.
[39] Australian Government—Bureau of Meteorology. *Monthly Mean Daily Global Solar Exposure Sydney Olympic Park AWS (Archery Centre)*. Accessed: Jul. 20, 2021. [Online]. Available: http://www.bom.gov.au/climate/data/index.shtml

HUYNH A. D. NGUYEN (Member, IEEE) received the B.E. degree in mechatronics engineering from Can Tho University, Vietnam, in 2009, and the M.Sc. degree in mechatronics engineering from the University of Siegen, Germany, in 2015. He is currently pursuing the Ph.D. degree with the Faculty of Engineering and Information Technology, University of Technology Sydney (UTS), Australia. He has been working as a Lecturer and a Researcher with the Department of Automation Technology, Can Tho University, since 2010. He has been the Vice Chair of the UTS IEEE Student Branch, since 2021. His research interests include IoT technology, data processing and analysis, machine learning, and deep learning.

QUANG P. HA (Senior Member, IEEE) received the B.E. degree in electrical engineering from the Ho Chi Minh City University of Technology, Ho Chi Minh City, Vietnam, in 1983, the Ph.D. degree in complex systems and control from the Moscow Power Engineering Institute, Moscow, Russia, in 1993, and the Ph.D. degree in intelligent systems from the University of Tasmania, Australia, in 1997. He is currently an Associate Professor with the Faculty of Engineering and Information Technology, School of Electrical and Data Engineering, University of Technology Sydney, Australia. His research interests include automation, robotics, and control systems. He has been on the Board of Directors of the International Association of Automation and Robotics in Construction, since 2007. He was a recipient of a number of best paper awards from the IEEE, IAARC, and Engineers Australia, including the Sir George Julius Medal, in 2015. He was the conference chair/the co-chair of several international conferences on automation and intelligent systems. He has been on the Editorial Board of the IEEE TRANSACTIONS ON AUTOMATION SCIENCE AND ENGINEERING (2009–2013), *Mathematical Problems in Engineering*, and *Electronics*. He is currently an Associate Editor of *Automation in Construction* and *Robotica*.